Small angle neutron scattering investigation of structural inversion in a three-component ionic micro-emulsion

1991 J. Phys.: Condens. Matter 3 F91

(http://iopscience.iop.org/0953-8984/3/42/009)

J. Phys.: Condens. Matter 3 (1991) F91–F107. Printed in the UK

Small angle neutron scattering investigation of structural inversion in a three-component ionic micro-emulsion

S H Chen†, S L Chang†, R Strey‡ and P Thiyagarajan§

† Department of Nuclear Engineering and Center of Materials Science and Engineering, 24–211, Massachusetts Institute of Technology, Cambridge, MA 02139, USA

‡ Max-Planck Institut für Biophysikalische Chemie, Postfach 2841, D–3400 Goetingen, Federal Republic of Germany

§ Intense Pulsed Neutron Source, Argonne National Laboratory, Argonne, IL 60439, USA

Received 20 May 1991

Abstract. We have made an extensive investigation of the phase diagrams and the associated micro-structure of a pseudo-ternary system AOT/water (0.6 wt% NaCl)/decane. This micro-emulsion system shows, for a surfactant concentration in excess of 6 wt%, a characteristic phase progression from a water-in-oil (W/O) micro-emulsion in coexistence with excess water at low temperatures to an oil-in-water (O/W) micro-emulsion in coexistence with excess oil at high temperatures through a one-phase micro-emulsion in the intermediate temperatures. Thus, one expects a structural inversion to occur somewhere in the one-phase channel. We have performed extensive small angle neutron scattering (SANS) measurements to study the pathway of such a structural inversion in this micro-emulsion system when there are comparable amounts of oil and water in the system, and when the volume fraction of water is much higher than that of oil. In the former case, we observed the inversion of the W/O to the O/W micro-emulsions through an intermediate bicontinuous one-phase micro-emulsion. In the latter case, we show that the inversion takes place through a pathway of L_3–L_α–L_1 as temperature increases. Particular emphasis is put on analyses of the interfacial structure in different micro-emulsion phases.

1. Introduction

In a recent paper [1], we have demonstrated the continuous inversion from a W/O micro-emulsion at low temperatures to an O/W micro-emulsion at high temperatures within the one-phase channel of AOT/water (0.6 wt% NaCl)/decane micro-emulsion system by small angle neutron scattering (SANS). At constant AOT (an ionic surfactant sodium-bis-ethylhexylsulpho-succinate) weight fraction γ, of 12%, a continuous structural evolution as a function of temperature has been shown to take place as the O/W weight fraction α is varied from 15 to 90% [2]. At low O/W weight fractions ($\alpha = 15$ and 20%), the micro-emulsion has been shown to transform from a water domain in oil continuous environment at low temperatures to oil droplets in water at higher temperatures through an intermediate region of a lamellar phase (L_α). On the other hand, at equal oil and water volume fractions ($\alpha = 40\%$), the structural transformation was shown to go through an intermediate state of a bicontinuous micro-emulsion

0953-8984/91/420F91+17$03.50

within the one-phase channel which occurs at hydrophile–lipophile balanced (HLB) temperature [1]. In this article, we extend our investigation to even smaller contents of oil and surfactant ($\alpha = 10\%$, $\gamma = 8\%$) and demonstrate that the lower arm of the isotropic one-phase channel is in fact an L_3-phase. The phase behaviour and scattering properties are consistent with the bilayer structure of the surfactant layer with the hydrophobic part being swollen by the oil. We also determine the interface structure of the lamellar phase at the intermediate temperature. Finally, conclusive evidence is given for the droplet structure of the high-temperature one-phase O/W micro-emulsion.

The L_3-phase is a liquid isotropic phase characterized by an observable streaming birefringence and opalescence; both properties increase upon dilution. It may be found in a large variety of systems [3–10], and it is always observed in the vicinity of a highly dilutable lamellar phase (L_α). Indeed, it has been shown recently that the bilayers comprising the dilute lamellar phase are very much the same as those in the L_3-phase.

Experimentally, a transition from a lamellar to an L_3-phase in the water-rich regime is always observed when the surfactant is rendered more hydrophobic. In general, an ionic amphiphile, and in particular AOT, can be made to change from being lipophilic to hydrophilic by raising the temperature. This occurs because the fractional dissociation of the counter-ion will increase when the temperature is increased. On the other hand, addition of NaCl has exactly the opposite effect. It would make AOT less hydrophilic, because the salt ions would compete with the counter-ion and the head groups for the water of hydration. This combination of NaCl addition and raising the temperature can be used to tune the phase behaviour of AOT/water (ϵ% NaCl)/decane micro-emulsion systems with precision [11, 12]. For example, an addition of 0.6 wt% NaCl to water allows the general pattern of the phase behaviour of an ionic amphiphile-water–oil micro-emulsion system to be observed [12, 2]. Figures 1 and 2 show the phase diagrams of an AOT/D_2O(0.6 wt% NaCl)/decane system in terms of their projections on T–γ (constant α) and T–α (constant γ) planes. Figure 1(a) is the T–γ projection at $\alpha = 40\%$ and figure 1(b) is the T–α projection at $\gamma = 12\%$. Figure 2(a) is the T–γ projection at $\alpha = 10\%$ and figure 2(b) is the T–α projection at $\gamma = 8\%$.

Theoretically, the L_α to L_3 transition has been explained in various ways [12–17] which involve a change in the spontaneous curvature of the surfactant layers. On lowering the temperature, there is a tendency for each surfactant monolayer comprising the bilayer to curve toward water, which induces a transition from L_α to L_3. In this transition, there is a free energy gain due to the change in topology: there are more interconnecting passages for the surfactant bilayers in the L_3-phase.

Thus, the inversion of the micro-structure across the lamellar phase with increasing temperature is intuitively expected for the AOT/water (0.6 wt% NaCl)/decane micro-emulsion system. At low temperatures, one finds an L_3-phase, where the surfactant bilayers, swollen by oil, wrap around water domains forming a bicontinuous structure; at somewhat higher temperatures, an L_α-phase, where the surfactant bilayers stretch out into more or less flat sheets, is found; with further increase of temperature, the lamellar sheets bulge and break up into polydisperse oil droplets dispersed in a continuum of water. A very schematic evolution of the micro-structure with increasing temperature is depicted in figure 3. The hatched area represents oil-swollen surfactant bilayers (L_3 and L_α) or monolayers (L_1), and the white portion in the figure represents the water domain.

In section 2, we briefly summarize some of the relevant experimental parameters for the subsequent discussion. In section 3, we formulate various models used for

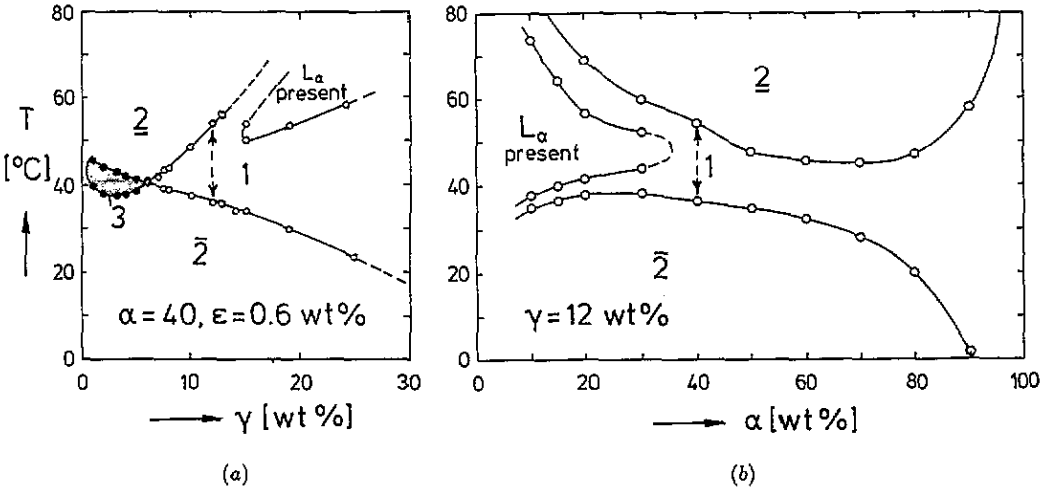

Figure 1. Sections through the body of heterogeneous phases in the phase prism of AOT/D_2O(0.6 wt% NaCl)/decane micro-emulsion system. (*a*) The diagram is a section at $\alpha = 40\%$ showing the relative positions of $\bar{2}$,2 and 1 phase regions in the T–γ plane. (*b*) A section at $\gamma = 12\%$ in the T–α plane.

the analyses of SANS data. This is followed by a discussion of the results of the analyses, which lead to the determination of the structural parameters, in section 4. Section 5 summarizes the results of the SANS experiment and proposes a possible future extension.

2. Experiment

2.1. Materials

The amphiphile AOT was obtained from Fluka and purified according to the procedure developed by Shinoda and Kunieda [18]. Sodium-bis-hexylsulphosuccinate, the short chain homologue of AOT, was obtained from Henkel (Düsseldorf) and was used as purchased. D_2O was obtained from Merck and is quoted to be 99.75% isotopically pure. n-decane was obtained from Merck (> 99.0%).

2.2. Sample preparation

Samples were prepared by weight, first dissolving AOT in the decane at an elevated temperature, then adding brine. The NaCl concentration, $\epsilon = 0.6$ wt%, was kept constant. We use the notation α = (wt decane)/(wt decane + wt D_2O), γ = (wt AOT)/wt of solution).

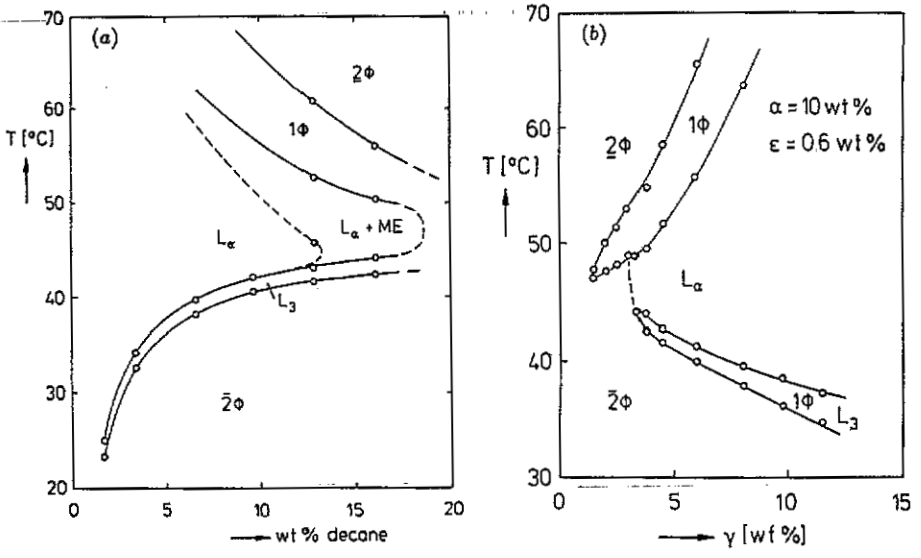

Figure 2. Sections through the body of heterogeneous phases in the phase prism of AOT/D_2O(0.6 wt% NaCl)/decane micro-emulsion system. (*a*) A section at $\gamma = 8\%$ in the T–α plane. (*b*) The diagram is a section at $\alpha = 10\%$ showing the relative positions of $\bar{2}$, $\underline{2}$ and 1 phase regions in the T–γ plane as well as the extent of the dilute lamellar phase L_α. The lower one-phase region is characterized by a strong opalescence and streaming birefringence and is termed the 'anomalous' or L_3-phase.

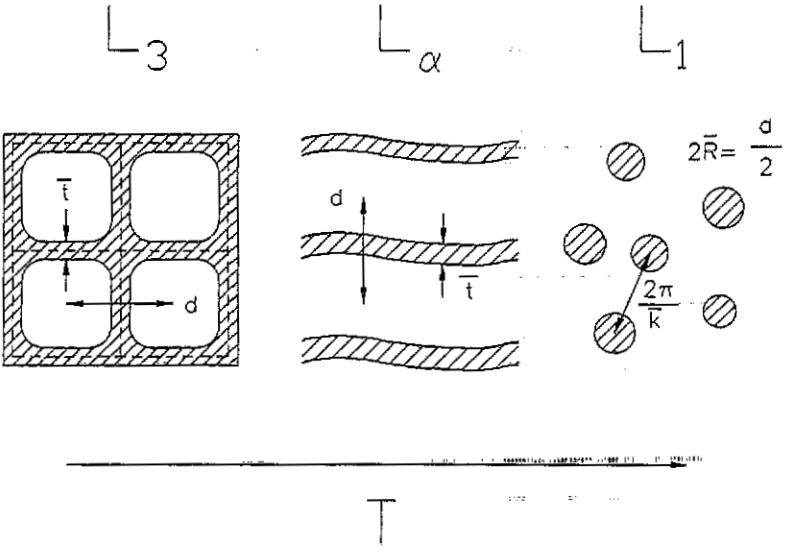

Figure 3. Schematic evolution of the micro-structure of the micro-emulsions from L_3- to L_α- to L_1-phases with increasing temperature.

2.3. Phase diagram determination

The phase diagrams shown in figures 1 and 2 were determined by starting at high γ and diluting with brine and oil at constant α. For a given composition, the number and type of phases were determined visually in a thermostatic water bath. Crossed polarizers were used to detect an isotropic lamellar phase and the streaming birefringence of the L_3-phase. As previously described in detail, this procedure yields sections through the phase prism (see figure 4 of [2]).

2.4. Electrical conductivity measurement

The conductivity was measured using a Wayne Kerr Autobalance Bridge (B 905) operating at 1 kHz. The cell constant $a = 0.736$ cm^{-1} was determined using 0.01D KCl. The increase in electrical conductivity caused by the increase in mobility of the ions as a function of temperature is estimated by using a reference solution. The reference is made from brine (0.6 wt% NaCl in D_2O) and a short chain homologue (sodium-bis-hexylsulpho-succinate) of AOT. This short chain surfactant forms only small micelles. The concentration was chosen to be equimolar to that of the AOT in solution, without oil added. The electrical conductivity is a sensitive indicator of an obstruction effect. In figure 4 we show the electrical conductivity κ as a function of temperature for a solution with $\alpha = 10\%$ and $\gamma = 8\%$. For comparison, the conductivity of the reference solution has been drawn to demonstrate that, in the range of the L_α-phase, there is a considerable obstruction [19] due to a one-dimensional lamellar structure, whereas at high temperature there is no detectable obstruction.

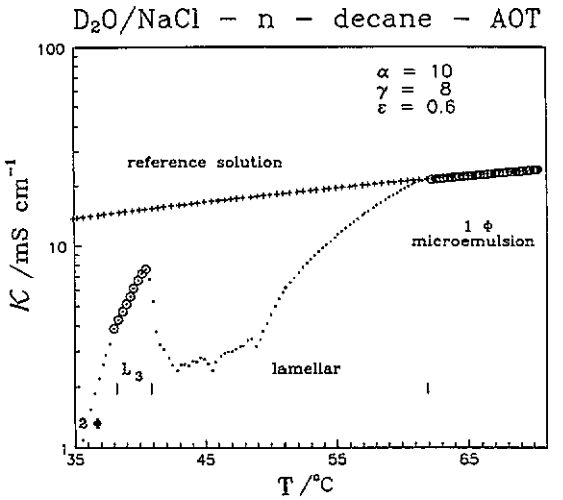

Figure 4. Electrical conductivity as a function of temperature for the AOT/D_2O(0.6 wt% NaCl)/decane micro-emulsion system at $\alpha = 10\%$ and $\gamma = 8\%$. For comparison, the conductivity of a reference solution is also shown to demonstrate that in the range of the L_3-phase, there is a considerable obstruction due to the bilayer-type structure. At high temperature there is no such obstruction detectable indicating the presence of globular or tubular structures.

2.5. SANS measurement

The first sample of AOT/D_2O(0.6 wt% NaCl)/D-decane with $\alpha = 40\%$ and $\gamma = 12\%$ was measured at the Riso National Laboratory, Denmark. The experimental setup and data analysis procedure have been described in [1]. The second sample of AOT/D_2O(0.6 wt% NaCl)/H-decane with $\alpha = 10\%$ and $\gamma = 8\%$ was measured at the SAD1 spectrometer at the Intense Pulse Neutron Source at the Argonne National Laboratory. This time-of-flight SANS spectrometer uses polychromatic incident neutrons with a wavelength distribution λ between 1.5 and 12 Å, emerging from a liquid hydrogen source. The measurements cover a fixed Q-range from 0.006 to 0.35 $Å^{-1}$ without having to move the position-sensitive detector. Each measurement took 1 h using a 1 mm thick quartz sample cell. The data reduction and normalization followed the standard procedure described in the user's manual of SAD1 [20]. In this article $I(Q)$, where $Q = (4\pi/\lambda)\sin(\theta/2)$, θ being the scattering angle, denotes an absolute scattering cross section per unit volume of the sample, having a dimension cm^{-1}.

3. Models

Molecular mixtures of surfactant, water and oil can be regarded as a pseudo-two-component system to a good approximation from the point of view of neutron scattering. We use D_2O for the water which has a scattering length density, $\rho_{D_2O} = 6.363 \times 10^{10}$ cm^{-2}. The oil component has a scattering length density of a typical hydrocarbon, $\rho_{oil} = -0.4888 \times 10^{10}$ cm^{-2}. The surfactant component can be partitioned between the water and the oil: the ionic head groups are heavily hydrated and can be incorporated into part of the water, and the hydrocarbon tails can be blended into the oil. For AOT, we may write the volume fraction of the head group φ_H as $\varphi_H = \alpha\varphi_s$, and that of the tail φ_T as $\varphi_T = (1-\alpha)\varphi_s$, where $\alpha = v_H/v_s = 65/611$ and φ_s is the volume fraction of the surfactant. The natural way of analysing scattering from two-component isotropic random structures, such as micro-emulsions, is to use the Debye correlation function $\Gamma(r)$ [21]. The scattering intensity $I(Q)$ can be written as a three-dimensional Fourier transform of the Debye correlation function:

$$I(Q) = \langle\eta^2\rangle \int_0^\infty dr\, 4\pi r^2 j_0(Qr)\Gamma(r) \tag{1}$$

where $\langle\eta^2\rangle = \varphi_1\varphi_2(\rho_{D_2O} - \rho_{oil})^2$ is the mean square fluctuation of the local scattering length density and $\varphi_1 = \varphi_{D_2O} + \varphi_H$ and $\varphi_1 = \varphi_{oil} + \varphi_T$ are the volume fractions of the major and minor components of the system respectively. The Debye correlation function, which is defined as the normalized local scattering length density autocorrelation function, has clear boundary conditions where $\Gamma(0) = 1$ and $\Gamma(\infty) = 0$. However, the most important property that is relevant to micro-emulsions is a condition on the first derivative of $\Gamma(r)$ [22]:

$$\Gamma'(r=0) = -\frac{1}{4\varphi_1\varphi_2}\frac{S}{V}. \tag{2}$$

S/V denotes the total inter-facial area per unit volume of the sample and is given to a very good approximation by $S/V = \varphi_s/\Delta$, where $\Delta = v_s/a_H$. v_s is the volume of the surfactant molecule and a_H is the area per molecule that the head group subtends at the water–oil interface. This quantity Δ can be experimentally measured using the absolute intensity of large Q portion of $I(Q)$ curve [2].

3.1. Debye correlation function for the oil-water (bulk) contrast case

To analyse the second sample which is AOT/D_2O(0.6 wt% NaCl)/H-decane with $\alpha = 10\%$ and $\gamma = 8\%$, we shall use a generalized Teubner–Strey (TS) model. The Debye correlation function in this case is

$$\Gamma_{TS}(r) = j_0(kr)\exp(-r/\xi). \tag{3}$$

The Fourier transform of $\Gamma_{TS}(r)$ in equation (1) gives $I(Q) = \langle\eta^2\rangle S(Q)$. The structure factor $S(Q)$ is given by

$$S(Q) = \frac{8\pi/\xi}{a^2 - 2bQ^2 + Q^4} \tag{4}$$

where $a^2 = (k^2 + 1/\xi^2)^2$ is a positive quantity, and $b = k^2 - 1/\xi^2$ can be a positive or negative depending on the relative magnitude of $d = 2\pi/k$ and ξ. In the original article by Teubner and Strey [23], b was assumed to be positive leading to a peak in $I(Q)$ occurring at $Q_{max} = b^{1/2}$. This implies that the two lengths are related by $\xi > d/2\pi$. We shall see in the following section that scattering intensity distributions in the L_3-phase show no distinct peak and are consistent with $\xi < d/2\pi$, hence b is negative. This is possible when the gradient square term in the Landau expansion of the free energy functional has a coefficient C_1 which is positive (normal case) [23].

3.2. Debye correlation function for the interface contrast case

To analyse the first sample, which is AOT/D_2O(0.6 wt% NaCl)/D-decane with $\alpha = 40\%$ and $\gamma = 12\%$, we shall use the modified Berk (MB) model [1, 24]. This model is applicable to the situation when the scattering length densities of oil and water are matched and the scattering only comes from surfactant monolayers. In this model, the Debye correlation function $\Gamma_I(r)$ can be written in the form [1]:

$$\varphi_T(1 - \varphi_T)\Gamma_I(r) = \frac{1}{2\pi}\sin^{-1}[\tau(r;\overline{k},\nu)] + \sum_{n=1}^{N} C_n[\tau(r;\overline{k},\nu)]^n \tag{5}$$

where the coefficient C_n is given by

$$C_n = \frac{1}{\pi n! 2^n}\{[e^{-\beta^2}H_{n-1}(\beta) - e^{-\alpha^2}H_{n-1}(\alpha)]^2 - H_{n-1}^2(0)\} \tag{6}$$

and $H_n(x)$ is the Hermite polynomial. α and β are two parameters specifying the lower and upper clipping levels of the basic random waves used in the Cahn simulation scheme [24–26]. They are related to the volume fraction of the aqueous phase and the surfactant tails by $\varphi_1 = [1 - \mathrm{erf}(\beta)]/2$ and $\varphi_T = [\mathrm{erf}(\beta) - \mathrm{erf}(\alpha)]/2$ respectively. For the first sample, these equations give $\alpha = -0.1437$, $\beta = 0.01649$. The function $\tau(r;\overline{k},\nu)$ in equation (5) is defined as

$$\tau(r;\overline{k},\nu) = \int_0^\infty \mathrm{d}k f(k)\cdot j_0(kr)$$

where $f(k)$ is the distribution function of the wavenumber used in the simulation and $j_0(kr)$ is the autocorrelation function of a random cosine wave of wavenumber

k. In this article we choose the distribution of wavenumber to be an inverse Schultz distribution $f_{is}(k)$ given by

$$f_{is}(k) = \frac{[(\nu-2)\overline{k}]^{\nu-1}}{\Gamma(\nu-1)} \cdot k^{-\nu} \exp[-(\nu-2)\overline{k}/k]. \tag{7}$$

In this distribution, the parameter $\overline{k}$ is the first moment and ν specifies the dispersion of k around $\overline{k}$, specifically $\Delta k/\overline{k} = 1/(\nu-3)^{1/2}$. We choose this particular form of the distribution because it is zero at $k = 0$ and at large k it decays like a power law $k^{-\nu}$, which is necessary to fit SANS data. This MB model is also applicable to the bulk contrast case [26, 27]. The Debye correlation function in this case is also given by equation (5) with the factor $\varphi_T(1-\varphi_T)$ replaced by $\varphi_1(1-\varphi_1)$ and the constant α set equal to minus infinity in the coefficient C_n given in equation (6). In the latter case, the value of the single constant β in equation (6) is given by $\varphi_1 = [1+\mathrm{erf}(\beta)]/2$ [1].

3.3. Asymptotic model applicable to the analysis of large-Q data

When Q is large compared with the inverse of the coherent length of the micro-structure in a micro-emulsion, the scattering intensity distribution reflects the Fourier transform of the shortest distance scale micro-structure. For example, in the interface contrast case of the bicontinuous micro-emulsion, this portion of the intensity distribution reflects the monolayer structure of the surfactant film. On the other hand, in the L_3- and L_α-phases, the same portion of the intensity distribution can be analysed to obtain the thickness and its associated polydispersity of the oil-swollen bilayer.

The scattering intensity for a system of isotropic, randomly distributed monolayers or bilayers of an average thickness t suspended in a solvent (this can be a mixture of D_2O and deuterated decane, D-decane, or just D_2O), when the interference effect is negligible, can be written as

$$I(Q) = \frac{N}{V}(\Delta\rho)^2(At)^2\overline{P}(Q). \tag{8}$$

In writing down equation (8), we imagine that we divide the total interface area in the sample volume of V into N units of disk-like objects each having a cross-sectional area $A = \pi R^2$ and a thickness t. A should be chosen so that it is the area within which the layer can be considered to be flat. $\Delta\rho$ is the scattering length density difference between the hydrophobic part of the layers and the solvent. The particle structure factor for a randomly oriented disk, $\overline{P}(Q)$, can be written generally as

$$\overline{P}(Q) = \int_0^1 \mathrm{d}\mu \left[j_0\left(\frac{Qt\mu}{2}\right)\right]^2 \left\{\frac{2J_1[QR(1-\mu^2)^{1/2}]}{QR(1-\mu^2)^{1/2}}\right\}^2 \tag{9}$$

where μ is the cosine of the angle between the cylindrical axis of the disk and the $\overline{Q}$ vector of the scattering. If Q_{min} is the minimum Q for which the interference effect is negligible and if R is such that $Q_{min}R > 10$ and t is much smaller than R, then for those Q-ranges for which $Q > Q_{min}$, the integration in equation (9) has an appreciable value only when the value of μ is close to unity. Under this circumstance, we can set

$\mu = 1$ in the factor involving spherical Bessel function and pull it out of the integral sign. Then, the orientationally averaged particle structure factor reduces to

$$\overline{P}(Q) = \left[j_0\left(\frac{Qt}{2}\right)\right]^2 \frac{2}{Q^2R^2}\alpha(QR)$$

where the factor $\alpha(QR)$ is an integral very close to unity for $QR > 10$. In practice these assumptions are valid for a typical case where $R \simeq 1000$ Å and $t < 100$ Å. In order to be realistic, we need to further average the intensity distribution over a dispersion of the thickness t. It is easily shown, by substituting $\overline{P}(Q)$ into equation (8), that the resultant intensity is $I(Q) = 2\pi\varphi(\Delta\rho)^2Q^{-2}\langle \mathrm{tj}_0^2(Qt/2)\rangle$, where φ is the volume fraction of the disks. This is a familiar expression for the intensity of scattering from disk-like objects [28], except for the appearance of the average over the thickness distribution. In carrying out the average of the last factor, we can conveniently take a Schultz distribution for the thickness, namely, $f_s(t) = \{[(Z+1)/\bar{t}]^{z+1}/\Gamma(Z+1)\}t^z \exp[-(Z+1)t/\bar{t}]$, where t is the average thickness and the dispersion around $\bar{t}$ is given by $\Delta t/\bar{t} = (Z+1)^{-1/2}$. The final expression for the intensity is

$$I(Q) = 4\pi\varphi(\Delta\rho)^2Q^{-4}\left(\frac{Z+1}{Z}\right)\frac{1}{t}[1 - (\cos\psi)^{Z-1}\cos(Z\psi)] \qquad (10)$$

where $\tan\psi = Q\bar{t}/(Z+1)$. It is easily seen from the small Q expansion of the cosine factors that equation (10) predicts a smooth crossover from Q^{-2} to Q^{-4} behaviour occurring at $Q\bar{t} \simeq 10$. We shall now use this expression to fit the large-Q portion of the SANS intensity distributions from monolayers in bicontinuous micro-emulsions having the interface contrast to demonstrate that we can extract the average thickness $\bar{t}$ and the dispersion $\Delta t/\bar{t}$.

Figure 5(a) shows SANS intensity distributions for the first sample AOT/D_2O (0.6 wt% NaCl)/D-decane taken at three temperatures, 37.8, 41.5 and 46.6 °C, near the structural inversion temperature (40 °C) previously determined [1]. The symbols are experimental data points and the full curves are results of the fits using equation (10). The fitting was made in the Q-range $0.04 < 0.25$ Å^{-1}. The minimum Q, 0.04 Å^{-1}, was chosen in such a way that the interference effect was negligible to the right of that value. Table 1 lists the fitted parameters for all the seven temperatures that we have investigated within the one-phase channel [1]. It can be seen from figure 5(a) that equation (10) fits the entire Q-range exceedingly well. The average thickness turns out to be $\bar{t} = 10.7 \pm 0.3$ Å with the associated dispersion $\Delta t/\bar{t} = 56\%$. In a previous contrast variation study of AOT micelles in an aqueous solution, it was determined that the hydrophobic tail of an AOT molecule has a fully stretched length of 12.6 Å [29]. Taking into account the oil penetration into the tail of the surfactant, the 10.7 Å we obtained for the monolayer thickness is quite reasonable. Figure 5(b) shows the same set of data shown in figure 5(a) fitted with the MB model [1] using equation (5) in conjunction with equation (1). This scheme allows us to use the fitted parameters $\bar{k}$ and ν to generate the three-dimensional micro-structure of the bicontinuous micro-emulsion [1, 26]. Figure 6 is the three-dimensional micro-structure generated in this way and its planar cut through the equator of the cube. The white contours represent the surfactant monolayers and the dark region represents the contrast matched D_2O and D-decane. Visually the contour thickness distribution is not inconsistent with the polydispersity of 56% as deduced from the fitting with the asymptotic model.

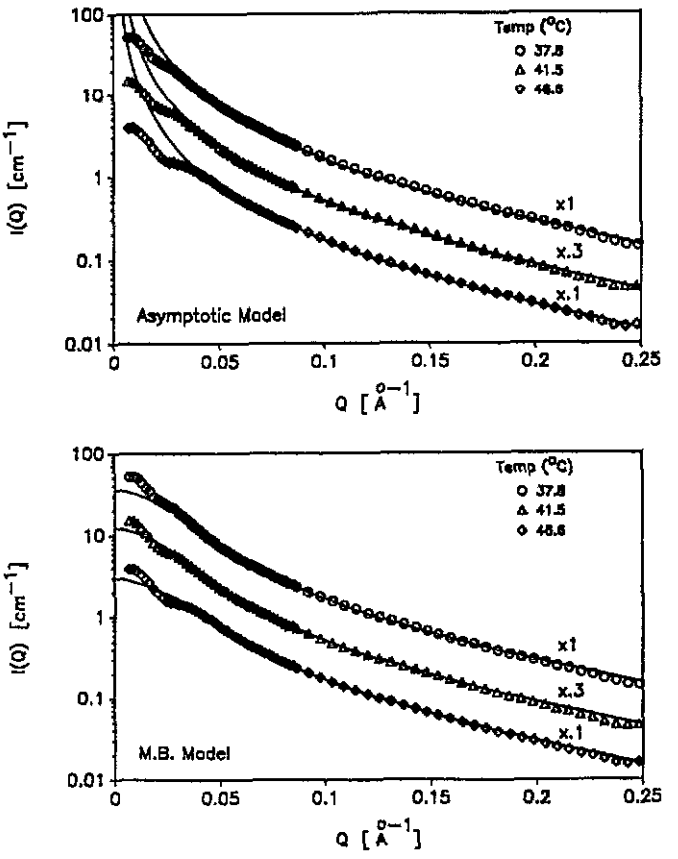

Figure 5. SANS intensity distributions of the interface contrast case, in an absolute scale, for the first sample, AOT/D_2O(0.6 wt% NaCl)/D-decane, at three temperatures, 37.8, 41.5 and 46.6 °C. Symbols represent the experimental data points and the full curves are the fitted results from (*a*) the asymptotic model and (*b*) the modified Berk model.

4. Structural inversion of the water-rich micro-emulsion

In this section, we discuss the results of analyses of SANS data from the second sample, AOT/D_2O(0.6 wt% NaCl)/H-decane, which has a composition $\alpha = 10\%$ and $\gamma = 8\%$. In section 2, we have already given the electrical conductivity data for this sample as a function of temperature. The phase boundary between the W/O two-phase micro-emulsion and the L_3-phase micro-emulsion occurs at 38 °C. We see from figure 4 that the conductivity rises sharply on entering the L_3-phase and this increase suddenly stops as the sample enters the L_α-phase at 40 °C [see figure 2(*a*)]. This can be interpreted as indicating that the micro-structure of the L_3-phase is bicontinuous and as it makes transition to the L_α-phase at 40 °C, the obstruction effect of the lamellar sheets causes the conductivity to decrease. The transition from the L_α- to the L_1-phase occurs at 62 °C and from there on the conductivity approaches that of the reference solution. Thus, it can be inferred from this fact that the micro-structure of the L_1-phase is a collection of surfactant-coated oil droplets dispersed in water. The main point to demonstrate here is that in both the L_3- and L_α-phases, the micro-

Table 1. Asymptotic model parameters for AOT/D_2O(0.6 wt% NaCl)/D-decane bicontinuous micro-emulsion.

Temp (°C)	$\bar{t}$ (Å)	$\Delta t/\bar{t} = (Z+1)^{-1/2}$	χ^2	Intensity factor A
37.8	10.41	56%	0.001	1.01
39.9	10.88	56%	0.001	1.00
41.5	10.86	56%	0.001	1.01
44.0	10.57	56%	0.001	1.02
46.6	10.58	56%	0.002	1.01
47.9	10.78	56%	0.004	1.02
50.0	11.01	56%	0.006	1.02

Composition: $\alpha = 40\%$, $\gamma = 12\%$, $\varphi = 8.98\%$, $\Delta\rho = 6.15 \times 10^{10}$ cm^{-2}.

$$\chi^2 = \frac{1}{N-1}\sum_{i=1}^{N}\frac{(I_{\mathrm{exp},i} - I_{\mathrm{theo},i})^2}{I_{\mathrm{exp},i}} \qquad Q\text{-range fitted: } 0.04 < Q < 0.25 \text{ Å}^{-1}$$

$$I_{\mathrm{theo}} = A4\pi\varphi(\Delta\rho)^2 Q^{-4}\left(\frac{Z}{Z+1}\right)\frac{1}{\bar{t}}[1 - (\cos\psi)^{z-1}\cos(Z\psi)] \qquad \text{where } \tan\psi = Q\bar{t}/(Z+1).$$

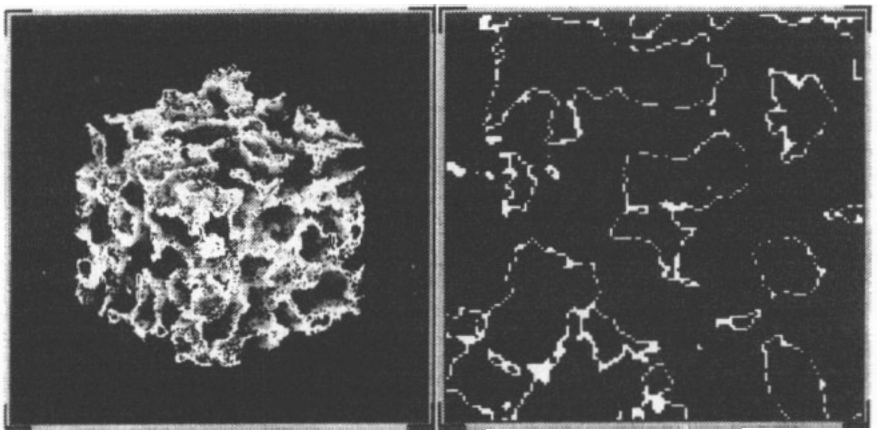

Figure 6. Simulated three-dimensional picture and its planar cut through the equator of the cube for the first sample (AOT/D_2O(0.6 wt% NaCl)/D-decane, $\alpha = 40\%$ and $\gamma = 12\%$) at $T = 41.5$ °C. The white contours represent the surfactant monolayers and the dark region represents the contrast matched D_2O and D-decane.

structure of the micro-emulsion consists of oil-swollen surfactant bilayers dispersed in water, but in the L_1-phase it is surfactant-monolayer-coated oil droplets dispersed in water. We shall first show this evidence by analysing the SANS data using the asymptotic model. Figure 7 gives a plot of a dimensionless intensity, $Q^4I(Q)(\Delta\rho)^2\bar{t}$, against a dimensionless wavenumber, $(Q\bar{t})^2$. According to equation (10), this curve should depend only on Z and the volume fraction of the hydrophobic component φ. This plot should show a transition from an initially linear relation at small Q to a constant at large Q as $I(Q)$ makes the transition from Q^{-2} to Q^{-4} behaviour. In this figure the open circles represent the data from the L_α-phase at 46 °C and the open triangles those from the L_3-phase at 38 °C. The full curves are the calculated results from equation (10). The parameters of the fits are shown in table 2. It is to be

emphasized that this is a comparison between the calculated and measured intensity on an absolute scale. The agreement in absolute terms is indicated by the amplitude factor A being 1.00 ± 0.01. The overall fits are excellent with χ^2 value of 0.002. The striking fact revealed by this fit is that the thickness of the bilayer $\bar{t}$ is 69.0 ± 5 Å for both temperatures, indicating the similarity of the short-range structures of L_3 and L_α. The large-scale structures will be discussed later. The polydispersity of the thickness is of the order of 50%. We have also made an attempt to fit the data at 65 °C, in the L_1-phase, by this model. This is indicated in the third row of table 2. Although an apparent fit can be achieved, the amplitude factor cannot be made less than 2.2, which is far beyond the confidence level of the absolute intensity calibration. We can, however, fit the 65 °C data satisfactorily with a polydispersed spherical oil droplets model [2] as shown in the last row of table 2. The mean diameter $2\bar{R}$ turns out to be 113 Å with a dispersion $\Delta R/\bar{R} = 36\%$. Alternatively, we can also fit the high-temperature data with the MB model in the bulk contrast (equations (5) and (6) with $\alpha = -\infty$ and $\beta = 0.602$). We obtain a satisfactory fit to the SANS data in the Q-range $0.02 < Q < 0.25$ Å^{-1} with the inverse Schultz distribution parameters (see section 3.2) $\bar{k} = 0.0356$ Å^{-1} and $\Delta k/\bar{k} = 40\%$. We may interpret $\bar{d} = 2\pi/\bar{k} = 176.5$ Å to represent the average inter-droplet distance and $\Delta k/\bar{k}$ the fluctuation around this mean distance. Using these two parameters, we can generate a three-dimensional micro-structure of this droplet micro-emulsion. The structure is shown in figure 8 together with its planar cut through the equator of the cube. A detailed inspection of figure 8 shows that the average size of the droplets is about 100 Å with a size dispersion of about 50% and the inter-droplet distance of the order 200 Å. These values are consistent with our interpretation of the fitted parameters using the polydisperse droplet model.

Table 2. Asymptotic model parameters for AOT/D_2O(0.6 wt% NaCl)/H-decane sample.

Temp (°C)	$\bar{t}$ (Å)	$\Delta t/\bar{t} = (Z+1)^{-1/2}$	χ^2	Intensity factor A
38	69.88	53%	0.012	1.00
46	69.11	50%	0.022	1.01
65	111.5	41%	0.016	2.20

Polydispersed sphere model: $I(Q) = A\frac{4\pi\varphi}{3}(\Delta\rho)^2\left[\frac{(Z+6)(Z+5)(Z+4)}{(Z+1)^3}\right]\bar{R}^3\frac{\langle R^6\bar{P}(QR)\rangle}{\langle R^6\rangle}$

65 °C $\quad 2\bar{R} = 113$ Å $\quad \Delta R/\bar{R} = 36\%$ $\quad \chi^2 = 0.008$ $\quad A = 1.07$

Composition: $\alpha = 10\%$, $\gamma = 8\%$, $\varphi = 19.71\%$, $\Delta\rho = 6.85 \times 10^{10}$ cm^{-2}

Q-range fitted: $0.04 < Q < 0.25$ Å^{-1}

Modified Berk model

65 °C $\quad \bar{k} = 0.0356$ Å^{-1} $\quad \Delta k/\bar{k} = 40\%$ $\quad A = 1$

4.1. Generalized Teubner–Strey model

Finally, we apply the generalized TS model described in section 3.1 in an attempt

Table 3. Generalized TS model parameters for AOT/D_2O(0.6 wt% NaCl)/H-decane sample.

Temp (°C)	Δ (Å)	d (Å)	ξ (Å)	$\Delta(4\varphi_1\varphi_2/\varphi_s)$	$2b$ ($\times 10^{-4}$)	$d/2\pi\xi$	χ^2	Intensity factor A
38	7.02	522	62.7	62.8	−2.18	1.32	0.54	0.97
39	7.00	487	61.2	62.6	−2.00	1.26	0.43	0.98
46	7.00	359	67.6	62.6	+1.75	0.85	0.39	0.96
65	7.64	243	71.7	68.3	+9.50	0.54	0.85	1.02

$$I(Q) = (\Delta\rho)^2\varphi_1\varphi_2\frac{8\pi/\xi}{a^2 - 2bQ^2 + Q^4} \qquad \Gamma_{TS} = j_0\left(\frac{2\pi r}{d}\right)\exp(-r/\xi)$$

$$a^2 = \left[\left(\frac{2\pi}{d}\right)^2 + \frac{1}{\xi^2}\right]^2 \qquad b = \left(\frac{2\pi}{d}\right)^2 - \frac{1}{\xi^2}$$

Composition: $\alpha = 10\%$, $\gamma = 8\%$, $\varphi_1 = 0.803$, $\varphi_2 = 0.197$, $\varphi_s = 0.071$, $\Delta\rho = 6.85 \times 10^{10}$ cm^{-2}

Q-fitted: $0.006 < Q < 0.25$ Å^{-1}

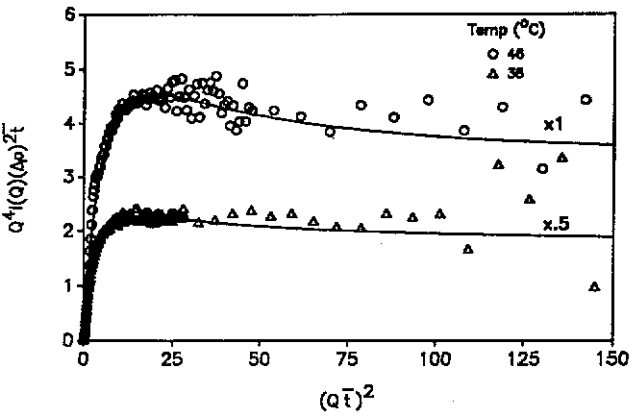

Figure 7. A plot of the dimensionless intensity $Q^4I(Q)(\Delta\rho)^2\bar{t}$ against the dimensionless wavenumber $(Q\bar{t})^2$ for the second sample, AOT/D_2O(0.6 wt% NaCl)/H-decane, with two temperatures, 38 and 46 °C. The open circles represent the data from the L_α-phase at 46 °C and the open triangles those from L_3-phase at 38 °C. The full curves are the fitted results from the asymptotic model.

to fit the SANS data over their entire Q-range. Figure 9(a) shows $I(Q)$ against Q plots for three sets of data in the order of increasing temperature from 38 to 46 to 65 °C. The symbols are the experimental points and the full curves are the calculated results of the generalized TS model. Figure 9(b) has the same sets of data represented in $\log I(Q)$ against $\log Q$ plots. The generalized TS model is seen to fit all three cases very well except for the highest temperature case for $Q < 0.01$ Å^{-1}. There is a possibility that the rising intensity for $Q < 0.01$ Å^{-1} in this case is due to a spurious effect in the measurement. Or, it could be due to the possibility that these oil droplets are percolating. The fitted parameters are summarized in table 3. The first point to notice is that the coefficient b changes sign from positive to negative when crossing into the L_3-phase from the L_α-phase. Physically, this is a result of the

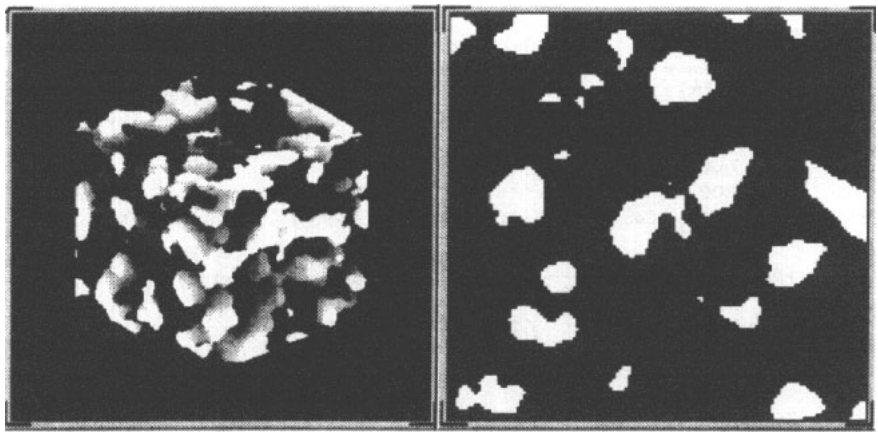

Figure 8. Simulated three-dimensional picture and its planar cut through the equator of the cube for the second sample (AOT/D_2O(0.6 wt% NaCl)/H-decane, $\alpha = 10\%$ and $\gamma = 8\%$) at $T = 65\,^{\circ}C$. The white region represent the polydispersed oil droplets, coated with surfactant monolayers, and the dark region represents D_2O.

disappearance of the scattering peak at finite Q upon the crossing into the L_3-phase. For a normal bicontinuous micro-emulsion with an equal volume fraction of oil and water, the parameter ξ is greater than $d/2\pi$ [2, 27]. In this case, the mean curvature of the surfactant film is zero. But in the L_3-phase, even though the micro-structure is bicontinuous, the surfactant film on each side of the bilayer curves toward water. This might be the reason for the change of sign of b.

We now turn to the interpretation of the two lengths d and ξ. For the highest temperature case, where we have previously shown that the micro-emulsion consists of polydispersed oil droplets of an average diameter 113 Å dispersed in water. According to the expression for the Debye correlation function in the TS model, equation (3), the first zero crossing of the distance distribution function [30] $p(r) = 4\pi r^2 \Gamma_{TS}(r)$ occurs at $r_0 = d/2$. One may interpret r_0 to be the maximum dimension of the droplets which is the diameter. $d/2$ in this case is seen to be equal to 122 Å, from table 3, agreeing with our previous estimate of 113 Å from the polydisperse sphere fit. For the intermediate temperature case at 46 °C in the L_α-phase, $d = 359$ Å from table 3 should be interpreted as the repeating distance within the lamellar stack. From the volume fraction consideration, this repeating distance d should be equal to $\bar{t}$ divided by φ_2 (volume fraction of oil plus surfactant tail). Taking $\bar{t} = 69.11$ Å from the previous estimate and $\varphi_2 = 0.197$, we get $d = 351$ Å, in agreement with the d deduced from the TS model. Finally, for the two lower temperature cases, 38 and 39 °C, in the L_3-phase, the average d is 500 Å. This should be interpreted as the average distance between the two water compartments next to each other wrapped around by the oil-swollen surfactant bilayer of an average thickness $\bar{t}$. Referring to the schematic drawing for the micro-structure of the L_3-phase in figure 3, we can write $\varphi_1 = (d - \bar{t})^3/d^3$. Combine this with the known surface-to-volume ratio $S/V = \varphi_s/\Delta = 6(d - \bar{t})^2/d^3$, we get a relationship

$$d = \frac{6\Delta\varphi_1^{2/3}}{\varphi_s}. \tag{11}$$

Taking the experimental values $\Delta = 7.02$ Å, $\varphi_s = 0.071$ and $\varphi_1 = 0.803$, we get from

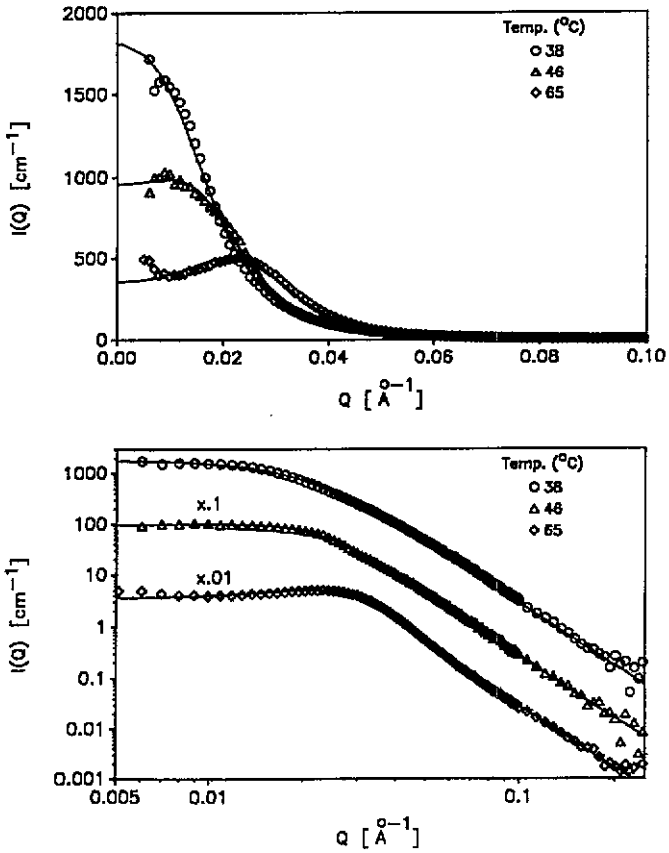

Figure 9. (*a*) SANS intensity distributions $I(Q)$, in an absolute scale, for the second sample, AOT/D_2O(0.6 wt% NaCl)/H-decane, at three temperatures, 38, 46 and 65 °C. Symbols represent the experimental data points and the full curves are the calculated results using the generalized TS model. (*b*) The same sets of data in the log–log plot.

equation (11) a value $d = 513$ Å, again in reasonable agreement with the TS model parameter.

As to the meaning of the parameter ξ, it is best interpreted as a quantity related to the inverse of the surface-to-volume ratio. Using equation (2) combined with $S/V = \varphi_s/\Delta$, we can easily obtain a relation $\xi = \Delta(4\varphi_1\varphi_2)/\varphi_s$. Since Δ can be directly determined from the SANS data at large Q, independently of the precise absolute intensity calibration, the product $\Delta(4\varphi_1\varphi_2)\varphi_s$ can be calculated independently. This is given in the fifth column of table 3. We are pleased to find that this product agrees with the fitted ξ values to within 10%, which is below the uncertainty of the determination of Δ. In the context of a discussion with regard to the micro-structure of bicontinuous micro-emulsions, we have previously concluded [26] that the ratio $d/2\pi\xi$ is a measure of the polydispersity of domain sizes in the system. As can be seen from the seventh column of table 3, this ratio increases as the temperature is lowered from the droplet phase at 65 °C down to the L_3-phase at 38 °C. This trend again coincides with values of $\Delta t/\bar{t}$ and $\Delta R/\bar{R}$ given in table 2 for the corresponding cases.

5. Conclusion

We have shown that the asymptotic model we derived in equation (10) can be used to extract a reliable average thickness and the dispersion of monolayers and bilayers in micro-emulsions. This model was first tested against a bicontinuous micro-emulsion with equal water and oil volume fractions at different temperatures and has yielded a correct monolayer thickness. The model was then applied to the case of a water-rich micro-emulsion in the L_3- and L_α-phases. We were able to show that in these two phases the micro-emulsion consists of oil-swollen bilayers suspended in a continuum of water. We next show that in the L_1-phase of the same micro-emulsion, the micro-structure consists of polydispersed oil droplets, coated with monolayers of surfactant, suspended in water. Thus, we demonstrated that the W/O micro-emulsion at low temperatures undergoes a structural inversion and transforms to an O/W micro-emulsion at higher temperatures through an intermediate lamellar structure. A generalized TS model was then applied to analyse the micro-emulsion in all three phases. The surprising result is that the coefficient b in the gradient square term of the Landau expansion of the free energy functional, in terms of the local order parameter $\psi(r)$, changes sign when the micro-emulsion is in the L_3-phase. This change of sign of b can also be realized in a lattice model of micro-emulsion formulated recently by Dawson [31] in the same region of the phase diagram. We gave physical meanings to the extracted parameters d and ξ in terms of the appropriate micro-structure of the micro-emulsion in different phases.

Our future plan is to further explore with SANS the micro-emulsion systems with $\gamma = 8\%$ but having a wide range of α, so that we can detect the crossover from the L_3-phase to the normal bicontinuous micro-emulsions as α increases from 10 to 40%. The coefficient b should change sign at this crossover.

Acknowledgments

This research is supported by grant form the Division of Materials Science of the Department of Energy, DE-FG01-90ER45429. We are grateful to IPNS of Argonne National Laboratory for providing us with neutron beam time and the SANS spectrometer for this experiment.

References

[1] Chen S H, Chang S L, Strey R, Samseth J and Mortensen K 1991 *J. Phys. Chem.* at press
[2] Chen S H, Chang S L and Strey R 1990 *J. Chem. Phys.* **93** 1907
[3] Fontell K 1975 *Colloidal Dispersions and Micellar Behavior (ACS Symposium Series 9)* (Washington DC: American Chemical Society) p 270
[4] Lang J C and Morgan R D 1980 *J. Chem. Phys.* **73** 5849
[5] Benton W J and Miller C A 1983 *J. Phys. Chem* **87** 4981
[6] Miller C A and Ghosh O 1986 *Langmuir* **2** 321
[7] Porte G, Marignan J, Bassereau P and May R 1988 *J. Physique* **49** 511
[8] Marignan J, Appell J, Bassereau P, Porte G and May R P 1989 *J. Physique* **50** 3553
[9] Gazeau D, Bellocq A M, Zemb T and Roux D 1989 *Europhys. Lett.* **9** 447
[10] Strey R, Schomacker R, Roux D, Nallet F and Olsson U 1990 *J. Chem. Soc. Faraday Trans.* **86** 2253
[11] Kahlweit M, Strey R, Firman P, Haase D, Jen J and Schomacker R 1988 *Langmuir* **4** 499

[12] Kahlweit M, Strey R, Schomacker R and Haase D 1989 *Langmuir* **5** 305
[13] Helfrich W 1978 *Z. Naturforsch.* A **33** 305
[14] Cates M E, Roux D, Andelman D, Milner S T and Safran S A 1988 *Europhys. Lett.* **5** 733
[15] Huse D A and Leibler S 1988 *J. Physique* **49** 605
[16] Porte G, Appell J, Bassereau P and Marignan J 1989 *J. Physique* **50** 1335
[17] Anderson D M, Wennerstrom H and Olsson U 1989 *J. Phys. Chem.* **93** 4243
[18] Kuneida H and Shinoda K 1980 *J. Coil. Interface Sci.* **75** 601
[19] Anderson D M and Wennerstrom H 1991 *J. Phys. Chem.* at press
[20] Epperson J E and Thiyagarajan P 1990 *SAD1 User's Manual* IPNS Argonne National Laboratory
[21] Debye P and Bueche A M 1949 *J. Appl. Phys.* **20** 518
[22] Debye P, Anderson Jr H R and Brumberger H 1957 *J. Appl. Phys.* **28** 679
[23] Teubner M and Strey R 1987 *J. Chem. Phys.* **87** 3195
[24] Berk N F 1988 *Phys. Rev. Lett.* **58** 2718
[25] Cahn J W 1965 *J. Chem. Phys.* **42** 93
[26] Chen S H, Chang S L and Strey R 1991 *J. Appl. Crystallogr.*
[27] Chen S H, Chang S L and Strey R 1990 *Progr. Colloid. Polym. Sci.* **81** 30
[28] Porod G 1982 *Small Angle X-ray Scattering* ed O Glatter and O Kratky (New York: Academic)
[29] Sheu E Y, Chen S H and Huang J S 1987 *J. Phys. Chem.* **91** 3306
[30] Glatter O 1979 *J. Appl. Crystallogr.* **12** 166
[31] Dawson K A 1991 private communication